

# Inscription of periodic modifications in glasses using IR-fs pulses: potential and applications

Stefan Nolte, Elodie Wikszak, Jens Thomas, Alexander Szameit, Felix Dreisow,  
and Andreas Tünnermann

Institute of Applied Physics, Friedrich-Schiller-University Jena  
Max-Wien-Platz 1, 07743 Jena, Germany  
nolte@iap.uni-jena.de; <http://www.iap.uni-jena.de>

## ABSTRACT

The use of ultrashort laser pulses has found widespread attention for the microstructuring of transparent materials. Specifically, the origin of refractive index changes in glasses and crystals was extensively investigated. This technique can be used for the direct-writing of waveguides along arbitrary paths into various transparent bulk materials. Moreover, evanescently coupled waveguides can be precisely produced using fs pulses, which allows to study the peculiar features of discrete diffraction and to provide the basis for two-dimensional soliton networks for all-optical switching and novel routing operations.

When extending the fs-writing technique to fibers, highly efficient Fiber Bragg Gratings (FBG) can be produced. Since this technology does not rely on photosensitivity, it is especially advantageous for applications in fiber lasers and amplifiers. The specific issues associated with the femtosecond inscription such as appropriate focusing and positioning techniques necessary for high quality FBG will be discussed. As an application example a fiber laser in a rare-earth doped fiber with integrated Bragg reflectors will be highlighted.

**Keywords:** ultrashort laser pulses, microstructuring, periodic structures, Fiber Bragg gratings, waveguides, integrated optics

## 1. INTRODUCTION

Within the past ten years, the use of ultrashort laser pulses for the localized modification within the bulk of transparent materials has attracted increasing interest.<sup>1,2</sup> When these intense pulses are tightly focused, the intensity in the focal volume can become high enough to initiate absorption through nonlinear field ionization (multiphoton absorption and tunneling ionization) and avalanche ionization. This nonlinear absorption results in the creation of an electron-ion plasma that is localized to the focal volume. As a consequence, permanent structural changes are induced.<sup>3</sup> Because the nonlinear absorption allows energy to be deposited into the bulk of a transparent material, these structural changes can be produced inside the sample without affecting the surface, allowing 3D structures to be fabricated by translating the laser focus through the sample.<sup>4-6</sup>

To date, three qualitatively different kinds of structural changes have been induced in the bulk of transparent materials with femtosecond laser pulses: at relatively low intensities an isotropic refractive index change can be created, which allows to guide light at relatively low losses;<sup>1,2,7,8</sup> at an intermediate intensity level a birefringent refractive index change is generated;<sup>9,10</sup> and voids are obtained at very high intensity levels.<sup>11-13</sup>

Within this paper we will focus on the realization of periodic structures at relatively low intensities, i.e. with isotropic refractive index changes. Within the first part of the paper this technology will be used to directly inscribe Fiber Bragg Gratings (FBG) within the core of doped and undoped fibers, while in the second part discrete systems based on a periodic structure transverse to the beam propagation direction will be fabricated and discussed.

## 2. INSCRIPTION OF FIBER BRAGG GRATINGS

Fiber Bragg Gratings (FBG) have become key components for optical telecommunication systems and sensor applications. They exhibit low losses and allow in-line spectral control of the guided light. Application examples include narrow-band reflectors and the use for the selective coupling of light into other existing fiber modes. This is achieved by a periodic variation of the refractive index in the fiber core. Within the past such gratings have been mainly fabricated with UV-Lasers in photosensitive materials.<sup>14-16</sup> However, highly doped rare earth fibers used in ‘state of the art’- fiber lasers possess material properties that make photosensitization difficult or impossible. Only few modifications have been reported recently in non photosensitive fibers based on two-photon absorption of 193 nm radiation.<sup>17,18</sup> This limitation can be overcome by using ultrashort pulses to inscribe the grating, because focused fs light can induce a local refractive index change even in non-photosensitive transparent material. Here, we will discuss two opportunities for the realization of FBGs with ultrashort pulses: the point-by-point<sup>19,20</sup> and the phase mask scanning technique.<sup>21-23</sup>

### 2.1. FBGs produced using the point-by-point technique

For the realization of the FBGs using the point-by-point technique laser pulses at 800 nm with a pulse duration of 50 fs (repetition rate 1 kHz), generated by an amplified Ti:sapphire laser system (Spectra-Physics, Spitfire), were focused by a 20x microscope objective with a numerical aperture of 0.35 into the core of a standard non-photosensitive single-mode silica fiber. The positioning of the fiber was realized using a high-precision 3D translation stage (Aerotech ABL9000) having a positioning accuracy of the order of 20 nm. Light of a broadband superluminescence diode is coupled into the fiber via a 50:50 coupler spliced to the fiber end for online monitoring. The light reflected from the fabricated FBG is measured using a spectrum analyzer at the other port of the coupler. A schematic of the experimental setup is shown in Fig. 1.

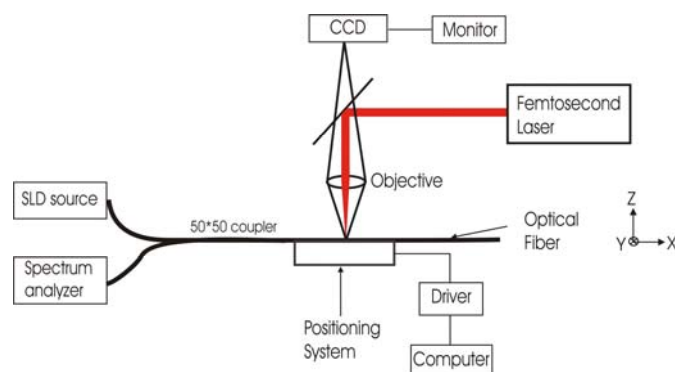


**Fig.1:** Schematic of the experimental setup for the inscription of FBGs using the point-by-point technique.

The width of the modifications induced into the fiber core is approximately  $2\ \mu\text{m}$  with a maximum refractive index change of  $1.2 \cdot 10^{-3}$ . Therefore, the shortest grating period which can be realized is  $2.1\ \mu\text{m}$ , which corresponds to the 4<sup>th</sup> reflection order for a wavelength of  $1.55\ \mu\text{m}$ . However, since the size of the fiber core ( $9\ \mu\text{m}$ ) is significantly larger than the induced modification, we decided to scan the laser beam perpendicular to the fiber axis for each position in order to generate a homogeneous refractive index plane throughout the core. The scan speed was  $0.5\ \text{mm/min}$ .

Figure 2 (left) shows the reflectivity spectrum obtained for a grating length of  $0.42\ \text{mm}$  at a period of  $2.1\ \mu\text{m}$ , i.e. corresponding to 200 periods. Apart from the main reflection peak at  $1520\ \text{nm}$  several secondary maxima are visible. With increasing grating length, these secondary maxima remain negligible and only the main reflection peak increases (see Fig. 2 (right) for a grating length of  $2.05\ \text{mm}$ , i.e. almost 1,000 periods).

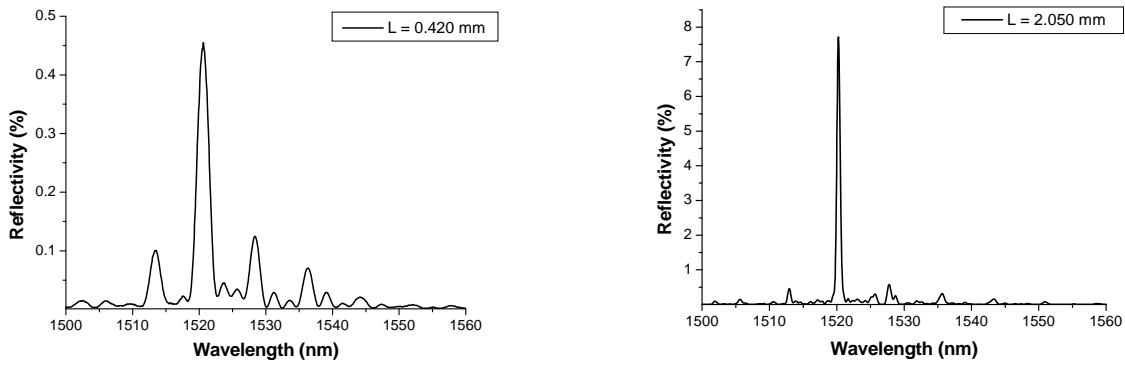


**Fig.2:** Evolution of the reflectivity spectrum with increasing grating length. Left: reflectivity spectrum for a grating length of 0.42 mm (i.e. 200 periods for the grating period of 2.1  $\mu\text{m}$ ); right: spectrum for a grating length of 2.05 mm.

The highest reflectivity we have obtained so far is 32 %. The grating length was 2.77 mm in this case and the reflected spectrum is shown in Fig. 3 (linear (left) and logarithmic scale (right)).

These results demonstrate the potential of this direct writing technology for the realization of FBGs in non-photosensitive fibers. It can be applied to various types of fibers and glasses, and due to the high flexibility of the process more advanced FBG-designs like chirped gratings or gratings with apodization can easily be realized.

However, the point-by-point technique possesses also some disadvantages. The spatial resolution of the induced modifications defines a minimum grating period requiring the use of higher order gratings. Moreover, a high precision positioning system is necessary in order to obtain the required grating homogeneity, which limits the grating quality. In addition, since each grating period is realized as a scanned line perpendicular to the fiber axis, the processing speed is relatively slow.

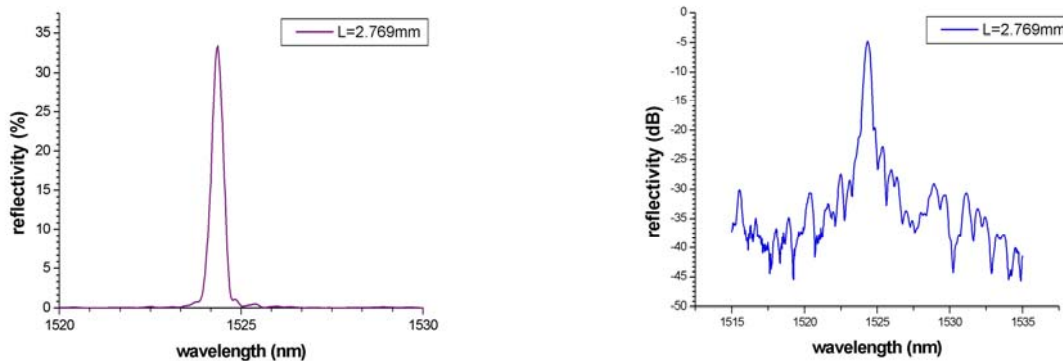


**Fig.3:** Reflectivity spectrum of a 2.77 mm long FBG (grating period 2.1  $\mu\text{m}$ ) fabricated using the point-by-point technique (left: linear scale; right: logarithmic scale).

## 2.2. FBGs produced using the phase mask scanning technique

In order to overcome the limitations arising from the point-by-point technique we studied the use of a phase mask to induce the grating into the fiber. In this case the periodic structure is due to the interference of the +1<sup>st</sup> and -1<sup>st</sup> diffraction orders of the phase mask grating. This yields a FBG with half the period of the phase mask grating.

The principal setup for the FBG inscription is shown in Fig. 4. We used a commercial fs laser system (Spectra Physics, Spitfire) with 50 fs pulses at a wavelength of 800 nm and a repetition rate of 1 kHz. The fs laser beam was focused laterally into the fiber with a cylindrical lens of  $f = 40$  mm. The phase mask has a period of  $2.15 \mu\text{m}$  resulting in a second order FBG for the design wavelength of  $1.55 \mu\text{m}$  (period  $1.075 \mu\text{m}$ ). It was placed between fiber and lens to obtain the periodic intensity pattern. For the positioning of the focused laser beam into the fiber core a high precision positioning system (Aerotech ABL9000) was used. In order to produce FBGs longer than determined by the area, where the two interference orders are overlapping, the fiber as well as the phase mask was translated simultaneously along the fiber axis with respect to the laser beam.

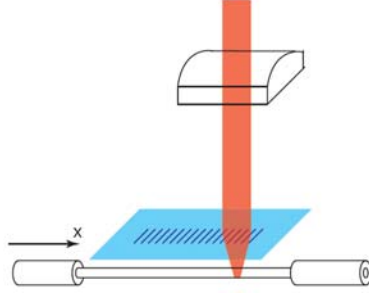


**Fig.4:** Schematic of the experimental setup for the inscription of FBGs using the phase mask scanning technique.

When working with cw or long-pulse lasers it is important that the energy contained in the  $0^{\text{th}}$  diffraction order of the phase mask is reduced to a few percent to avoid the formation of a parasitic periodical structure. In contrast, it is possible to obtain pure two beam interference with ultrashort laser pulses without such high requirements on the phase mask design due to the so-called order walk-off effect.<sup>24,25</sup> Since the different diffraction orders propagate with different angles they will arrive at different times in the observation plane (see Fig. 5). By choosing an appropriate distance between the phase mask and the fiber, the time difference between the  $1^{\text{st}}$  diffraction orders and the  $0^{\text{th}}$  order will be larger than the short coherence length of the laser. Therefore, the  $0^{\text{th}}$  order will be unable to interfere with the  $1^{\text{st}}$  orders and a pure two beam interference pattern is obtained.

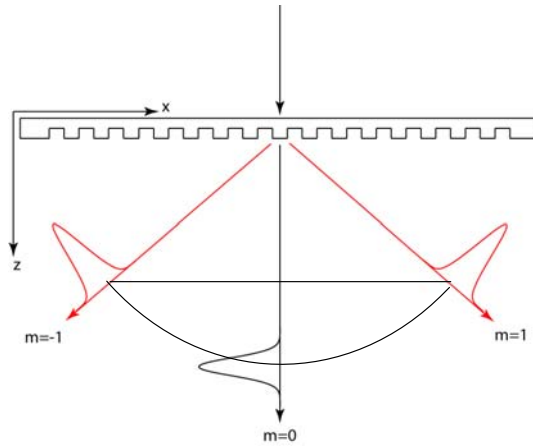


**Fig.5:** Due to the so-called order walk-off effect a pure two-beam interference pattern is obtained. Since the different diffraction orders propagate along different paths they will arrive at different times in the observation plane. Interference of the different orders is only possible if the path difference is shorter than the coherence length of the laser pulse.

The distance  $s_0$  between the phase mask and the fiber for which the order walk-off is sufficient can be described by

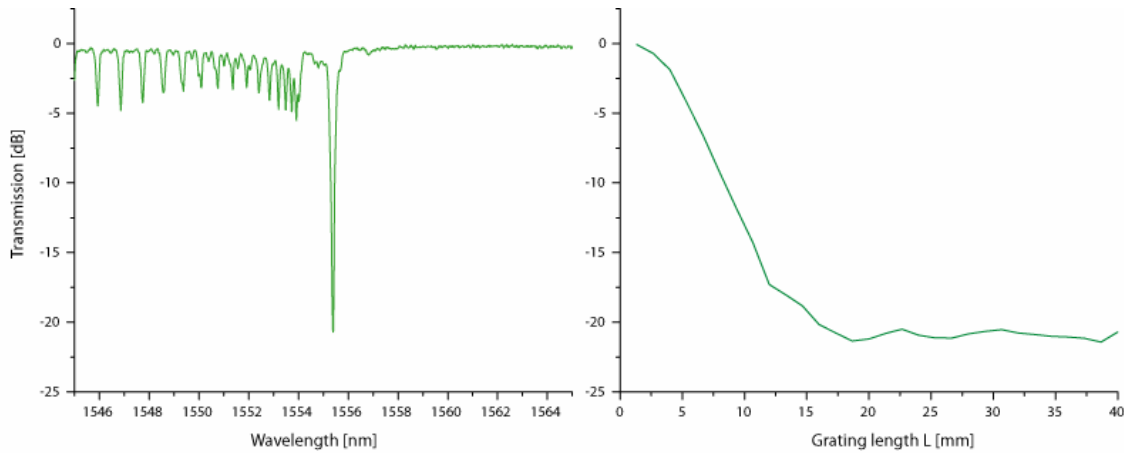
$$s_0 > \frac{l_{coh}}{1 - \cos \delta} \quad (1)$$

using the diffraction angle  $\delta$  and the coherence length  $l_{coh}$  of the laser.<sup>26</sup>

Another important issue is the appropriate focusing, since the refractive index modifications are induced only in the focal region due to nonlinear absorption. Thus, the focus has to be precisely located at the fiber core to successfully write a FBG. For high NA microscope objectives this can simply be achieved by choosing the appropriate distance between the lens and the fiber. When using a phase mask, however, high NA objectives cannot be used since a sufficient overlapping area of the diffraction orders has to be obtained. Thus, one has to rely on low NA cylindrical lenses for focusing. In this case the fiber curvature contributes a significant part to the focus formation. As simulations based on Gaussian optics reveal, the focus will never reach the fiber core for very low NA irrespective of the distance between lens and fiber.<sup>26</sup> However, for a Rayleigh range  $\rho$  of

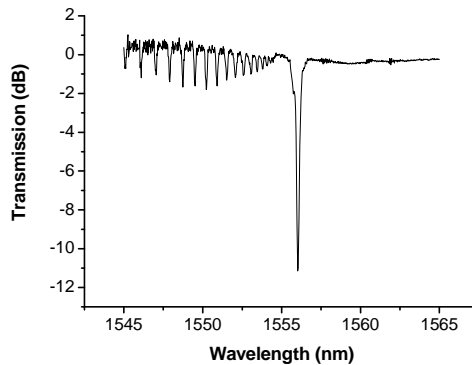
$$\rho = \frac{n \cdot r}{2(n-1)}, \quad (2)$$

where  $n$  is the refractive index and  $r$  the cladding radius of the fiber, the focus can just be positioned in the fiber core. One can show, that the requirements on position accuracy are significantly reduced in this case.<sup>26</sup> For our experimental conditions Eq. (2) is fulfilled by choosing a lens with a focal length of  $f = 40$  mm.



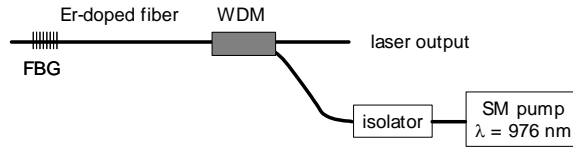
**Fig.6:** Transmission spectrum of a 2<sup>nd</sup> order FBG of 20 mm length (left). Right: evolution of the transmission at the Bragg wavelength as a function of grating length. The pulse energy was 600  $\mu$ J and the scan speed 4 mm/min.

Figure 6 (left) shows the transmission spectrum of a FBG (2<sup>nd</sup> order) of 20 mm length written into a standard telecommunication fiber (J-fiber, IG 09/125/250). The pulse energy was 600  $\mu$ J and the scan speed 4 mm/min in this case. The transmission is reduced by more than 20 dB at the Bragg wavelength. In the right part of Fig. 6 the development of the Bragg wavelength transmission is summarized as a function of grating length. As one can see, the transmission saturates for gratings longer than 20 mm.



**Fig.7:** Transmission spectrum of a 2<sup>nd</sup> order FBG of 40 mm length written in an Erbium doped fiber with a pulse energy of 500  $\mu$ J and a scan speed of 5 mm/min.

Such highly efficient FBGs can not only be produced in standard fibers but also in active fibers doped with rare-earth ions.<sup>27</sup> As an example Fig. 7 shows the transmission spectrum obtained in a single-mode Erbium doped fiber (Liekki ER80-8/150). The FBG (period 1.075  $\mu\text{m}$ ) is again a second order grating for the Bragg wavelength of 1550 nm with a length of 40 mm written with a pulse energy of 500  $\mu\text{J}$  and a scanning speed of 5 mm/min.



**Fig.8:** Schematic layout of the all integrated fiber laser.

Using this FBG as one cavity mirror an all-integrated fiber laser was set up (Fig. 8). The pump laser diode is coupled via a wavelength division multiplexer (WDM) coupler into the fiber core. The output cavity mirror is constituted from the 4 % Fresnel reflection of the perpendicularly cleaved end facet. The laser output characteristics are shown in Fig. 9. The slope efficiency is 31 % and the maximum output power obtained was 100 mW for a launched power of 375 mW. As no saturation was observed, higher pump powers should yield significantly higher output powers. The output spectrum has a FWHM bandwidth limited by the Optical Spectrum Analyzer resolution ( $< 0.06$  nm) and a signal to noise ratio of -45 dB.

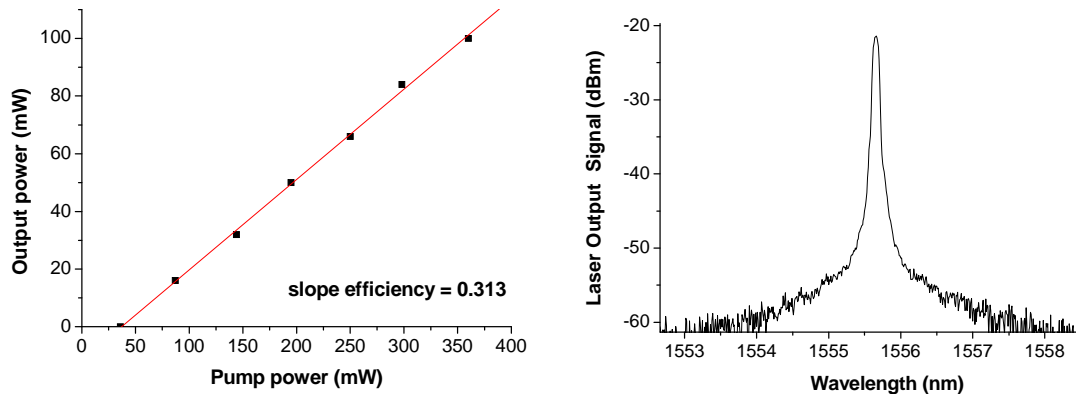


**Fig.9:** Output characteristics of the all integrated Erbium doped fiber laser. Left: output power versus pump power; right: output spectrum.

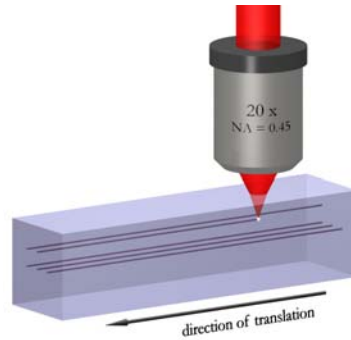
### 3. PERIODIC STRUCTURES TRANSVERSE TO THE BEAM PROPAGATION DIRECTION – DISCRETE SYSTEMS

So far the influence of a periodic structure along the waveguide on the optical properties has been discussed. Within this section a periodic structuring of the refractive index perpendicular to the propagation direction will be covered. In this case several waveguides are considered which are close enough together that light can couple from one waveguide to the other via the evanescent field. When the waveguides are arranged in a periodic lattice a discrete optical system is constructed exhibiting a significantly different propagation behavior than is found in isotropic materials.<sup>28,29</sup> As an example, diffractionless propagation is observed under certain illumination conditions in contrast to isotropic media where any beam will undergo diffraction.<sup>30</sup>

For the realization of such waveguide arrays in general the conventional techniques used in integrated optics are applied. This has the disadvantage that only planar arrays can be realized. However, two-dimensional waveguide arrays

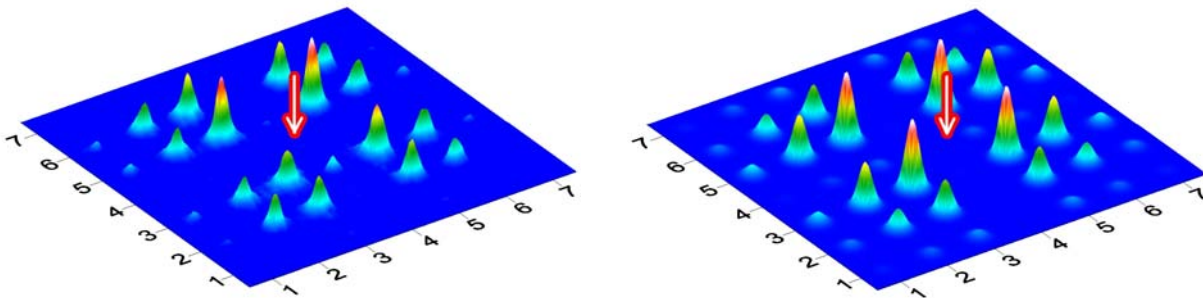
exhibit additional interesting properties. One possibility for the realization of such 2D waveguide arrays is the femtosecond laser direct writing technique.<sup>31,32</sup>

For the fabrication of the waveguide arrays, laser pulses at a wavelength of 800 nm with an energy of typically 0.3  $\mu$ J and a pulse duration of 50 fs (repetition rate 1 kHz), generated by an amplified Ti:sapphire laser system (Spectra-Physics Spitfire), were focused into a polished fused-silica sample. The focusing was accomplished by a 20x microscope objective with a numerical aperture (NA) of 0.45 (Zeiss Achroplan), which was corrected for a cover-glass thickness of 0.17 mm. By moving the sample transversally to the focus of the laser beam at typical speeds of 100  $\mu$ m/s waveguides are written (Fig. 10).



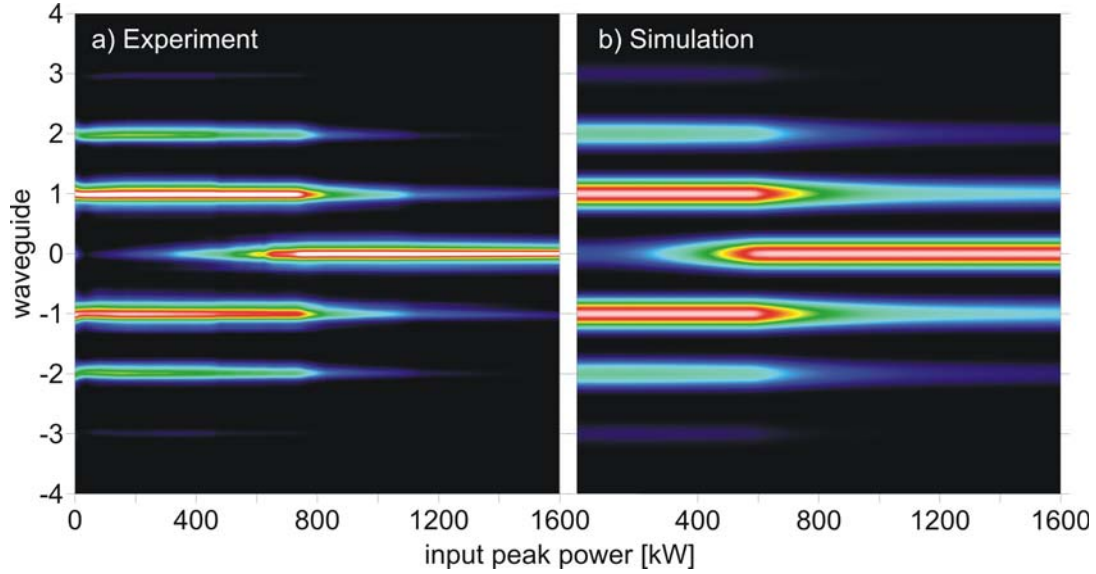
**Fig.10:** Schematic of the fabrication of a waveguide array using the femtosecond direct writing technique.

Figure 11 (left) reveals the intensity distribution at the output facet of a 7 x 7 cubic array with a waveguide length of 20 mm and a waveguide-to-waveguide separation of 25  $\mu$ m. Light at a wavelength of 740 nm has been launched into the central waveguide of the matrix (indicated by the arrow). The comparison with the numerical simulation for an ideal lattice is shown in Fig. 11 (right). There is excellent agreement with the experimentally recorded field distribution. Similar results are obtained when exciting the lattice at other waveguides (e.g. at the border or at the edge).<sup>31</sup> This proves the high quality of the waveguide lattice and its use for the investigation of discrete systems.



**Fig.11:** Intensity distribution at the exit of a 20 mm long 7 x 7 cubic waveguide array (waveguide separation 25  $\mu$ m) after excitation of the central waveguide with 740 nm light. Left: experimental result; right: simulation of an ideal array.

Apart from linear propagation nonlinear effects in discrete systems like the formation of discrete spatial solitons have attracted a lot of attention.<sup>28</sup> However, we recently observed that the nonlinearity of the glass matrix is significantly reduced due to the femtosecond laser structuring process. By analyzing self-phase modulation experienced by a short laser pulse propagating through a femtosecond written waveguide we were able to show that the nonlinear refractive index  $n_2$  was decreased up to only 25% of the value of the bulk material depending on the processing parameters.<sup>33</sup> Thus, when considering the design of a nonlinear discrete spatial lattice one has an additional degree of freedom by varying the nonlinearity of the material.



**Fig.12:** Light distribution at the exit of a planar waveguide array as a function of the incident peak power. At around 1,000 kW all light is confined in the central waveguide (which was excited). a) experiment; b) simulation.

Figure 12 shows a comparison between experiment (a) and simulation (b) of the nonlinear propagation within a planar waveguide array written by femtosecond pulses. The light distribution at the exit of the waveguide array is displayed as a function of the peak power of the laser pulse launched into the central waveguide. At a peak power around 1,000 kW self-focusing due to the nonlinear Kerr effect counterbalances the coupling between the waveguides and the light is localized in the central waveguide – a discrete spatial soliton is formed. Taking the induced changes in the nonlinear refractive index into account one can obtain perfect agreement between experiment and simulation.<sup>34</sup>

#### 4. CONCLUSION & OUTLOOK

In conclusion, the use of femtosecond laser pulses for the localized permanent modification of the refractive index within transparent media is a suitable tool for the fabrication of periodic structures. FBGs can be realized in various doped and undoped fibers without the necessity of photosensitivity. This offers the potential to fabricate them directly into active fibers and realize compact and stable fiber laser sources.

In addition this technique might be used for the fabrication of discrete optical systems. Here, the femtosecond direct writing technology has proven its high accuracy. Moreover, we have shown that this technique offers the potential not only to modify the linear but also the nonlinear optical properties.

#### 5. ACKNOWLEDGEMENTS

We acknowledge the Deutsche Forschungsgemeinschaft (DFG) for supporting this work.

## 6. REFERENCES

1. K. M. Davis, K. Miura, N. Sugimoto, and K. Hirao, *Opt. Lett.* 21, 1729 (1996).
2. K. Miura, J. Qui, H. Inouye, T. Mitsuyu, and K. Hirao, *Appl. Phys. Lett.* 71, 3329 (1997).
3. K. Itoh, W. Watanabe, S. Nolte, C. B. Schaffer, *MRS Bulletin* 31, 620 (2006).
4. W. Watanabe, T. Asano, K. Yamada, K. Itoh, and J. Nishii, *Opt. Lett.* 28, 2491 (2003).
5. S. Nolte, M. Will, J. Burghoff, and A. Tünnermann, *Appl. Phys. A* 77, 109 (2003).
6. A.M. Kowalewicz, V. Sharma, E.P. Ippen, J.G. Fujimoto, and K. Minoshima, *Opt. Lett.* 30, 1060 (2005).
7. S. Nolte, M. Will, J. Burghoff, A. Tünnermann, *J. Mod. Opt.* 51, 2533 (2004).
8. Y. Nasu, M. Kohtoku, and Y. Hibino, *Opt. Lett.* 30, 723 (2005).
9. L. Sudrie, M. Franco, B. Prade, and A. Mysyrowicz, *Opt. Commun.* 171, 279 (1999).
10. L. Sudrie, M. Franco, B. Prade, and A. Mysyrowicz, *Opt. Commun.* 191, 333 (2001).
11. E.N. Glezer, M. Milosavljevic, L. Huang, R.J. Finlay, T.-H. Her, J.P. Callan, and E. Mazur, *Opt. Lett.* 21, 2023 (1996).
12. E.N. Glezer and E. Mazur, *Appl. Phys. Lett.* 71, 882 (1997).
13. C.B. Schaffer, A.O. Jamison, and E. Mazur, *Appl. Phys. Lett.* 84, 1441 (2004).
14. G. Meltz, W. W. Morey, and W. H. Glenn, *Opt. Lett.* 14, 823 (1989).
15. K. O. Hill, B.Malo, F. Bilodeau, D. C. Johnson, and J. Albert, *Appl. Phys. Lett.* 62, 1035 (1993).
16. R. Kashyap, *Fiber Bragg Gratings*, Academic Press, New York, 1999.
17. J. Albert, M. Fokine, W. Margulis, *Opt. Lett.* 27, 809 (2002).
18. N. Grothoff, J. Canning, E. Buckley, K. Lyttikainen, and J. Zagari, *Opt. Lett.* 28, 233 (2003).
19. E. Wikszak, J. Burghoff, M. Will, S. Nolte, A. Tünnermann, and T. Gabler, "Recording of fiber Bragg gratings with femtosecond pulses using a point by point technique," in *Conference on Lasers and Electro-Optics*, 2004.
20. A. Martinez, M. Dubov, I. Khrushchev, and I. Bennion, *Electr. Lett.* 40, 1170 (2004).
21. S. J. Mihailov, C. W. Smelser, D. Grobnic, R. B. Walker, P. Lu, H. Ding, and J. Unruh, *J. Lightw. Techn.* 22, 94 (2004).
22. A. Dragomir and D. N. Nikogosyan, *Opt. Lett.* 28, 2171 (2003).
23. S. T. Slattey, D. N. Nikogosyan, and G. Brambilla, *J. Opt. Soc. Am B* 22, 354 (2005).
24. C. W. Smelser, D. Grobnic, S. J. Mihailov, *Opt. Lett.* 29, 1730 (2004).
25. C. W. Smelser, S. J. Mihailov, D. Grobnic, P. Lu, R. B. Walker, H. Ding, and X. Dai, *Opt. Lett.* 29, 1458 (2004).
26. J. Thomas, E. Wikszak, T. Clausnitzer, U. Fuchs, U. Zeitner, S. Nolte, and A. Tünnermann, *Appl. Phys. A* 86, 153 (2007).
27. E. Wikszak, J. Thomas, J. Burghoff, B. Ortac, J. Limpert, S. Nolte, U. Fuchs, and A. Tünnermann, *Opt. Lett.* 31, 2390 (2006).
28. H. Haus, L. Molter-Orr, *IEEE J. Quant. Electr.* 19, 840 (1983).
29. D. N. Christodoulides, F. Lederer, and Y. Silberberg, *Nature* 424, 817 (2003).
30. T. Pertsch, T. Zentgraf, U. Peschel, A. Bräuer, and F. Lederer, *Phys. Rev. Lett.* 88, 093901 (2002).
31. T. Pertsch, U. Peschel, F. Lederer, J. Burghoff, M. Will, S. Nolte, and A. Tünnermann, *Opt. Lett.* 29, 468 (2004).
32. A. Szameit, D. Blömer, J. Burghoff, T. Pertsch, S. Nolte, F. Lederer, and A. Tünnermann, *Appl. Phys. B* 82, 507 (2006).
33. D. Blömer, A. Szameit, F. Dreisow, T. Schreiber, S. Nolte, A. Tünnermann, *Opt. Express* 14, 2151 (2006).
34. A. Szameit, D. Blömer, J. Burghoff, T. Schreiber, T. Pertsch, S. Nolte, A. Tünnermann, and F. Lederer, *Opt. Express* 13, 10552 (2005).